Stable establishment of organ polarity several plastochrons before primordium outgrowth in Arabidopsis

Feng Zhao, Jan Traas

Laboratoire Reproduction et Développement des Plantes, Université de Lyon 1, ENS-Lyon, INRAE, CNRS, UCBL, 46 Allée d'Italie, 69364 Lyon, France

Authors for correspondence: Feng.Zhao@ens-lyon.fr; Jan.Traas@ens-lyon.fr

Key words: leaf polarity; Sussex signal; prepattern; laser ablation; Arabidopsis

Summary statement:

We revisited the classical surgical experiments in Solanaceae using precise laser ablations to explore the mechanism controlling organ dorsoventrality in vegetative and floral meristems in Arabidopsis.

Abstract

In many species, leaves are initiated at the flanks of shoot meristems. Usually, subsequent growth mainly occurs in the plane of the leaf blade, which leads to the formation of a bifacial leaf with dorso-ventral identities. In a classical set of surgical experiments in potato meristems, Sussex provided evidence that dorsoventrality depends on a signal emanating from the meristem centre. Although these results could be reproduced in tomato, this concept has been debated. We revisited these experiments in Arabidopsis where a range of markers are available to target the precise site of ablation. Using specific markers for organ founder cells and dorsoventral identity, we were unable to perturb the polarity of leaves and sepals long before organ outgrowth. While results in Solanaceae suggested that dorsoventral patterning was unstable during early development, we find that in Arabidopsis the local information contained within and around the primordium is able to withstand major invasive perturbations, long before polarity is fully established.

Introduction

Plant leaves can adopt a wide range of shapes and sizes depending on the species and the environment in which they develop. In many species, leaves initiate at the flanks of the shoot apical meristem as small bulges. In their most basic form, they then develop as flat, ellipsoid structures as growth mainly occurs in the plane of the leaf blade. In combination with a restricted expansion in the dorsoventral direction this leads to the formation of a thin leaf blade with functionally distinct abaxial and adaxial faces, pointing respectively away from and towards the stem, a property also referred to as leaf polarity.

Several genes have been associated with leaf shape and size, which are determined from the earliest stages of development onwards (e.g. Hervieux et al., 2016; Zhao et al., 2020; Zhu et al., 2020). Key are the regulators involved in setting up leaf polarity and which are activated before or during organ outgrowth. These include for example abaxial determinants such as FILAMENTOUS FLOWER (FIL) (Sawa et al., 1999; Siegfried et al., 1999) or KANADI1 (KAN1) (Kerstetter et al., 2001), adaxial determinants such as REVOLUTA (REV) or PHABULOSA (PHB) (McConnell et al., 2001) and the so-called margin genes including *PRESSED FLOWER (PRS)* and *WUSCHEL RELATED HOMEOBOX1 (WOX1)* (Scanlon et al., 1996; Nakata et al., 2012), expressed in the future leaf margin and in the middle domain separating the abaxial and adaxial domains. The network also involves regulation via small RNAs (Kuhlemeier and Timmermans, 2016). Some of the polarity genes are expressed very early, and in particular *REV* and *KAN1* might define a prepattern (Caggiano et al 2017) even before the upregulation of organ founder cell markers such as DORNROESCHEN-LIKE (DRNL) (Chandler et al., 2011) or ARABIDOPSIS PHOSPHOTRANSFER PROTEIN 6 (AHP6) (Besnard et al., 2014). If the regulatory network controlling polarity is impaired, leaf and leaf-like organs lose their bilateral symmetry and tend to become axisymmetric (Yamaguchi et al., 2012; Kuhlemeier and Timmermans, 2016).

How is the establishment of polarity coordinated? In a classical set of experiments, Sussex and co-workers used local incisions in potato meristems (Sussex, 1951; Kuhlemeier and Timmermans, 2016 for review). When an incision was made between the vegetative meristem and incipient leaf primordia, leaves did not flatten but developed into almost axisymmetric organs. This led to the hypothesis that leaf polarity depends on a signal coming from the meristem centre. This result was further consolidated in tomato (Reinhardt et al., 2005; Qi et al., 2014; Shi et al., 2017). Reinhardt et al (2005) showed that ablation in the epidermal L1 layer was sufficient to perturb leaf polarity, suggesting that the signal would require an intact surface layer. Interestingly, this layer is essential in the control of polarized auxin transport

during organ formation (Reinhardt et al., 2003; Kierzkowski et al., 2013) and the hormone has also been considered as part of the signal proposed by Sussex. Indeed certain mutants involved in auxin transport such as PINOID or PIN-FORMED1 develop axisymmetric lateral organs (Qi et al., 2014) and auxin transport generates differences in hormone concentrations between the periphery and the centre of the shoot apical meristem (de Reuille et al., 2006). Qi et al (2014) proposed that auxin could act as a reverse 'Sussex signal' flowing from the adaxial side of leaf primordium to the adjacent meristem to consolidate leaf dorsoventrality.

However, the concept of a single meristem-centred signal regulating leaf polarity has also been under debate. Although they were able to do so in *Epilobium hirsutum*, Snow and Snow could not confirm the ablation results in potato (Snow and Snow, 1954b). The traditional surgical experiments on meristems mostly rely on the morphology of young leaf primordia as the only marker to define the right position for incision. Snow and Snow therefore suggested that cuts leading to a loss in polarity inadvertently caused a reduction in size of the primordia in the radial direction which then led to abnormal development. More recently, several, more elaborated hypotheses have been brought forward to explain the processes leading to dorsoventrality (Husbands et al., 2009; Caggiano et al., 2017), although all of them require some form of meristem based signal or information. From a conceptual point of view, Koch and Meinhardt (1994) proposed a model which combined the existence of an organ inhibiting gradient around the meristem centre, with more local, self-organizing patterning processes within the initium itself as soon as the cells leave the inhibiting field. Although this has remained purely hypothetical, findings of Caggiano et al (2017) in Arabidopsis go into the direction of a more complex network of interactions involving auxin transport and pre-existing gradients of several transcription factors such as KAN1 and REV. The same authors performed a number of laser ablations between the meristem and incipient primordia and showed that the wounds inflicted by cutting can locally induce the expression of certain polarity genes such as *KAN1*. This result potentially questions the interpretation made by Sussex, as the loss of polarity observed in potato might be due to a wounding reaction involving the ectopic activation of abaxial determinants. However, in Arabidopsis, the organs were only followed in small vegetative meristems over short time frames after ablation and no organs with altered polarity were observed. We therefore decided to revisit the ablation experiments in *Arabidopsis thaliana*, using very early primordium and polarity markers. Performing ablations along or perpendicular to the radius of vegetative and floral meristems, we were unable to induce the formation of radialised leaves and sepals. This was even the case when the ablations were made two or three plastochrons (i.e. the time between successive leaf initiation) before organ outgrowth. Our results therefore support a model

where organ polarity does not require any meristem-based signal from the earliest stages of primordium specification onwards.

Results

Identifying precise targets for ablation using markers for founder cells and organ polarity

To identify the cell populations that would be ablated, we used a set of fluorescent markers for early organ development. For this purpose, we chose *pDRNL:erCERULEAN* as an organ founder cell marker (Chandler et al., 2011). In addition, we used *pFIL:erGFP*. This promoter is active in the abaxial domain of young outgrowing primordia and shows an extended expression in abaxialized mutants (Nakata et al., 2012; Tameshige et al., 2013). We also used *pPRS:SV40-3×GFP* to label the middle domain between both sides of the primordia (Scanlon et al., 1996; Nakata et al., 2012; Xu et al., 2015). Since the precise, relative expression dynamics of these markers has not been described, we constructed a set of lines co-expressing *pDRNL* with either *pFIL* or *pPRS*. To monitor cell growth and lineage, the membrane marker *pUBQ10:Lti6b-tdTomato* was included. In some experiments, propidium iodide (PI) was used for this purpose.

In the vegetative meristem, we followed organ initiation from I_3 (I_1 being the first incipient primordium that is ready to bulge out, and I_{1+n} the subsequent younger ones) to P_6 (P_1 designates the first visible outgrowing primordium and P_{1+n} the subsequent older ones). In complement to what has been described previously, *pDRNL* is active throughout the meristematic dome with a patchy pattern in the L2 and L3 layers (Fig.S1A-B). At the I_3 position however, *pDRNL* activity significantly increases and also becomes active in the L1 layer (Fig. 1A, Fig.S1A and Fig.S2). Lineage analysis shows that from I_3 to I_1, it covers both the future organ boundary and adaxial domain of the future primordium (Fig.1 and Fig. S2) i.e. a small group of about 5-6 cells in diameter. Slightly later than *pDRNL*, *pFIL* and *pPRS* driven signals become visible at I_1. They largely overlap with the *pDRNL* maximum, and no apparent polarization of these markers is distinguishable before P_1 when the primordia start to bulge out. At the P_1 stage, the activity of *pDRNL* and *pPRS* is more concentrated at the adaxial domain, while *pFIL* expression shifts to the abaxial domain and also partially overlaps with the middle domains. Slightly later on, at P_3, *pPRS* activity becomes restricted to the middle domain only. The polarized expression of the markers is fully resolved when the

primordium is clearly growing out and is about 3 cells high (P_4 in our experimental set-up). Note that *pPRS* signals are always extending more towards the lateral organ boundaries than the other two markers (Fig. 1, Fig. S1and S3).

Similar expression patterns of *pDRNL* and *pFIL* are found in the inflorescence meristem: *pDRNL* expression is visible from I_3 onwards, while *pFIL* initiates at I_1 (Fig. 2A, see also (Heisler et al., 2005; Refahi et al., 2021)). During early stage 2 of flower formation, *pDRNL* and *pFIL* expressions are restricted to the area where the cryptic bract slightly bulges out, but do not define a clear polarity. Both genes are switched off in the bract during late stage 2 of floral development. Until that moment, *pPRS* is only activated in a small number of individual nuclei, scattered randomly over the floral bud and as well as the entire inflorescence meristem (Fig. 2 and Fig. S3).

Soon after the inactivation of *pDRNL* and *pFIL* in the cryptic bract, the sepal primordia are specified. This is marked by a local activation of *pDRNL*, first in the outer (abaxial) and two lateral ones (Zhu et al., 2020). At late stage 2, *pDRNL* is activated in all 4 sepal primordia. Like in the vegetative meristem, it also covers the future boundary with the floral meristem. At floral stage 3 and 4, *pDRNL* activity becomes restricted to the adaxial side of the sepal primordia and is also expressed in a ring-like domain in one of the future inner whorls, probably corresponding to part of the third whorl (Fig. 2A-C). The activation of *pFIL* and *pPRS* is slightly later than *pDRNL* but still during late floral stage 2. As for the leaf, *pFIL* is initially activated at the sepal primordia in a pattern that is overlapping with *pDRNL*. At late floral stage 2, only the outer sepal is marked, followed by the inner and lateral sepals (see also Zhu et al., 2020) during stage 3. Like in the leaf primordia (Fig.1C-E and H), *pFIL* expression shifts peripherally during stage 3 and becomes limited to the abaxial and middle domains of the sepals at stage 4 (Fig. 2C-E, H and Fig. S3). *pPRS* is first activated in the outer sepal at late stage 2, partially overlapping with the *pDRNL* expression domain. Subsequently, *pPRS* is mainly expressed in the adaxial side of the sepal primordia. Gradually, *pPRS* becomes active in a ring covering the middle domain of all sepals as well as the lateral boundaries between them during stage 4 (Fig.2B, F-H, and Fig. S3).

In summary, while the staging of primordia can vary a little depending on the size of meristems, the relative expression-dynamics of the three different markers allow us to identify the precise moments when the organ founder cells and the different domains that characterize organ polarity are established. In this context, the upregulation of *pDRNL* marks the future organ boundary and adaxial domain, while in later stages *pFIL* marks the abaxial

domain and the middle domain, the latter being characterized in addition by *pPRS* expression. We next used these patterns to characterize the precise locations of the ablations. We distinguished two categories: (i) ablations that did not or only marginally touch the expression domains and (ii) ablations within specific domains of the initia or primordia. These will be discussed separately.

Ablations next to early leaf initia/primordia do not perturb leaf dorsoventrality in Arabidopsis

We first sought to repeat experiments where young primordia were physically separated from the central meristem through incision, which, in potato and tomato, resulted in the formation of abaxialized, axisymmetric organs. To this end, we performed circular ablations surrounding the meristem centre (i.e. perpendicular to the meristem radius) using *pDRNL* as an early leaf initium marker (Fig.3A). To exclude short distance signal transmission between meristem and the young leaves, the incisions were set as close as possible to the incipient primordia. In 12 meristems, 22 I_3 - I_1 primordia were left intact or only a few proximal cells were eliminated. In addition, we were able to follow 22 intact P_1 - P_2 in these meristems. Under these conditions, none of the leaves that grew out showed radial symmetry (Fig. 3, Fig.S4, S5, S6A-B). Even the ablations performed at I_3, when *pDRNL* was only just becoming upregulated and *pFIL* was not expressed at all (Fig.1A, Fig.S1C), polarized leaves grew out. Note that we could not determine whether there was any transient change in polarity. By any means, the patterning process did not require a meristem-based signal.

In tomato, not only incisions isolating the primordium from the central meristem cause a loss of dorsoventrality. In addition, incisions parallel to the meristem radius (i.e. at the lateral boundaries between organs) are sufficient to induce abaxialized organs (Shi et al., 2017).
In 2 I_2 and 5 I_1 initia, the ablations were 4-6 cells apart and left the initium (5-6 cells wide) intact or only slightly reduced its width. In all these 7 cases the resulting primordia showed a polarized distribution of *pDRNL* and *pFIL* signals 2-3 days after incision (Fig 4A, B). Finally, a characteristic leaf with dorsoventral identity formed 5 days after incision (Fig. 4C-D). Once the primordia had already started to bulge out, lateral ablations of 3 to 8 cells wide did not affect growth and leaf polarity (13/13 of P_1 and P_2) (Fig. S7).

Within the limits of the markers that we have used, we did not find any indication, that lateral ablations at the boundaries and ablations between the vegetative meristem and initiating organs perturbed polarity from I_3 onwards, i.e. before *pFIL* and *pPRS* are activated.

Laser ablations next to early sepal initia in the floral meristem do not perturb dorsoventrality in Arabidopsis

We next assessed the effect of laser ablation on sepal shape and polarity at the floral meristem. As for the vegetative meristem, circular ablations were used to isolate sepal initia from the central meristem. In 7/19 stage 2 floral buds, this led to an increase in sepal number, the remaining 12/19 had four sepals as in WT (Fig. 5A-D). None of the sepals were radial symmetric. This was even the case when early stage 2 flowers were ablated, i.e. before *pFIL* expression was activated (8/8 meristems, Fig. 5A-B, D).

We then confined sepal initia by two parallel ablations at the lateral boundaries in stage 2 floral buds. All 14 sepal initia established normal polarity and no radial sepals were formed (Fig. 5E-F).

In summary, in the floral meristems, neither parallel nor perpendicular ablations close to the initia could perturb dorsoventrality.

Ablations within the leaf initia/primordia are followed by the regeneration of dorsoventral organs or lead to growth arrest

As mentioned earlier, Snow and Snow (1954a) proposed that the incisions made by Sussex could have led to a reduction in size of the initia, and thus causing the formation of radialized leaves. We further sought to confirm this with a set of ablations where either the adaxial or abaxial domain of the initia/primordia was eliminated or initium/primordium width was reduced to only 1-4 cells.

Adaxial ablations. We also performed more restricted ablations, limited to an arc of the circumference, targeting single initia. These were sufficiently large to ablate up to the entire adaxial half of the *pFIL* expression domain. After ablation at I_1 or P_1, polarised leaves were formed (n=5, Fig. 6A-A'', Fig.S6C). This was correlated, however with an initial inactivation of *pFIL*, followed by a more distal reactivation of *pFIL* toward the meristem periphery, and adaxial cells regenerated from the abaxial side of the wound (Fig 6A-A''). Notably, this also involved a redefinition of the organ boundary with the meristem (Fig. 6A'-A'').

Abaxial ablations. 12 of the circular ablations described above went through I_3-I_1 initia eliminating the abaxial part of the *pDRNL* labelled domain (see Fig. S5 I_3 for an example of precise positions). In all cases growth arrest was observed. Some outgrowths occurred next to the wound, but these did not develop further and did not express *pDRNL* (Fig. 3A-B; Fig. S4). We also performed 6 more restricted ablations, limited to an arc of the circumference, targeting single initia. This resulted in an elimination of 60-80% of the entire *pFIL* domain just leaving a few cells adaxially. In these cases as well, the outgrowth of leaf primordia was halted, showing limited cell division of the remaining adaxial cells and loss of *pFIL* expression (Fig. 6B'-B'', Fig. S6C).

Lateral ablations. As we have seen, lateral ablations leaving most of the leaf primordia or initia intact, did not affect development. We next analyzed a set of lateral ablations at an early stage, eliminating a significant part of the founder cells. In 4 cases (at 2 I_1 and 2 I_2), the incisions were very close, i.e. 1-2 cells apart. These initia did not further develop and the signal of *pDRNL* or *pFIL* was lost (Fig.7A-B''). 13 ablations at I_1/I_2 were 3-4 cells apart. 7 of the resulting primordia then developed normally (Fig. S6C). In 6 cases, however, growth was dramatically reduced, leading to the formation of small bulges. Polarity in these primordia could be maintained for days. Later on, the abaxial *pFIL* marker extended adaxially (Fig. 7C-E'') in these small, non-growing primordia. This apparent loss of polarity could be due to indirect effects, may be related to their limited growth.

Ablations within the sepal initia do not perturb organ polarity

We next performed ablations on the floral meristem, restricted to an arc of the circumference, eliminating part of the sepal before they started to grow out. As a control, restricted ablations just next to the initium, did not perturb development, as was also observed for circular ablations (n=2, Fig. 8A-A' compare figure 5A-D). This was also the case when the adaxial part of the *pFIL* domain itself was killed (n=8, Fig. 8B-B').

When we performed lateral ablations eliminating part of the initia themselves and reducing their width, we could not observe any effect on polarity. Notably, even leaving one radial row of initium cells did not perturb sepal polarity, although the sepals were narrower (n=4, Fig. 8C-C').

We finally eliminated all founder cells of the outer sepal primordia. In 3/3 successful ablations, no sepal regenerated along the dorsal-ventral axis. To our surprise, however, flat sepals were reinitiated from the lateral boundaries, which was characterized by the ectopic activation of *pDRNL* in these domains (Fig. S8A). To test if the reactivation of *pDRNL* is induced by signals from the neighboring sepal primordia, we eliminated the founder cells of the outer and lateral sepal primordia in 5 floral buds. In all cases, *pDRNL* was activated in the lateral boundaries and new flat sepals developed (Fig.S8B). As shown above, the margin promoter *pPRS* is active in these lateral boundaries (Fig. 2). *PRS* plays a role in cell proliferation and is important for the lateral extension of sepals (e.g. Zhao et al., 2020). We therefore wondered if sepals would also regenerate from boundaries in mutants with a reduced margin activity. This was not the case and no regeneration was observed from the boundary, when the outer and lateral sepal primordia in *wox1 prs* double mutants were ablated (n= 5, Fig. S8C).

Discussion

In this study, we combined *in vivo* imaging with laser ablation to study the establishment of organ polarity in both vegetative and floral meristems. In particular the use of larger vegetative meristems grown in short days allowed us to monitor leaf development over long periods. This is an important advantage over previous work, where more precise lineage tracking was not possible.

We find that organ polarity does not require any meristem-based signal at least two or three plastochrons before the organs grow out, at a moment when *pDRNL* is upregulated and organ founder cells are selected. Likewise, sepal polarity becomes autonomous at stage 2 of flower development, i.e. when sepals are initiated, but haven’t started to grow.

Husbands et al (2009) proposed that leaf polarity is determined in three phases: establishment, resolution, and maintenance. The main players would be activated during the first phase, but not necessarily in the correct pattern, which would be defined during the second phase and maintained afterwards. While the first two phases would in principle require external information, local molecular regulation within and around the leaf primordium itself should be sufficient for maintenance once it is fully deployed. While results in tomato and potato suggested the dorsoventral patterning was not very robust during the initiation process itself (Sussex, 1951; Reinhardt et al., 2005), we show here that even at a stage when major regulators such as *FIL* or *PRS* are not yet activated, polarity is already robustly established and maintained. Indeed, although the ablations cause major changes in local signaling and

even can affect gene expression (Heisler et al., 2010; Caggiano et al., 2017; Zhao et al., 2019), we did not see any effect on leaf polarity, suggesting that an external signaling gradient is unlikely to play a role once *pDRNL* is activated. Further work is now required using additional markers, to show that there are no more subtle effects on ad/abaxial polarity.

To understand this early establishment of polarity, the results reported by (Caggiano et al., 2017) are particularly relevant. They showed the existence of concentric expression zones around the meristem centre of genes involved in organ polarity: a domain weakly expressing the adaxial determinant *REV* in the meristem centre, surrounded by cells expressing the abaxial gene *KAN1* at the meristem periphery. Both transcription factors mutually inhibit each other and the boundary between the two domains covers cells that have not yet been incorporated in new primordia, i.e. this boundary precedes organ formation. Both genes therefore seem to define some type of 'prepattern' for polarity. At sites where auxin accumulates, *REV* is further upregulated at least from I_2 onwards (Caggiano et al., 2017). Our data suggest that this upregulation is accompanied by increased *DRNL* expression as well, and there is evidence that both transcription factors directly interact (Chandler et al., 2007; Zhang et al., 2018). We hence deduce that initially, both REV and DRNL cover the future organ boundary and the adaxial domain. At a later stage, when tissue folding starts at the boundary, auxin levels go down. Combining our results with those of Caggiano et al, we propose that this would be followed by the inactivation of both *REV* and *DRNL* and the activation of *KAN1* in the forming organ boundary.

Caggiano et al., (2017) also suggested that the loss of polarity observed by Sussex (1951) after incision between the meristem and the young primordia could be the result of perturbation of this prepattern as a wound reaction. As we have shown here, ablations substantially modify meristem structure, causing local outgrowth. In addition, it has been shown that ablation can alter auxin fluxes, microtubule organisation, and gene expression patterns (Heisler et al., 2010; Caggiano et al., 2017; Zhao et al., 2019). In particular the polarity gene *KAN1* is induced by wounding. Caggiano et al suggested that this ectopic expression might create a zone of abaxial identity and organs formed in this zone would then be abaxialised. This might notably explain the loss in polarity observed in tomato and potato. We did not obtain any clear evidence for this scenario, as we never obtained abaxialised leaves or sepals after ablation. We did, however, observe changes in local patterning. When a large part of the future adaxial domain was eliminated, *pFIL* activity was initially lost, a new boundary was respecified and a polarized primordium was formed a bit further away from the wound after ablation (Fig. 6). This could indicate that the ablation leads to some type of dedifferentiation followed by local repatterning. No meristem-based signal would be required

for this process, as the initium was cut off by the ablation. It is possible that ectopically induced KAN1 expression would be sufficient to guide such a reprogramming.

By any means, the results on Arabidopsis are very different from what was reported on Solanaceae. A possible explanation for this discrepancy is that the expression dynamics and roles of polarity determinants differs between species. This is for example illustrated by small RNAs targeting auxin response factors (ARFs) which are rather implicated in the maintenance phase in the developing leaves of Arabidopsis, while they are indispensable for the establishment of polarity in several monocot species (see Kuhlemeier and Timmermans (2016) for discussion).

A final issue concerns the lateral organ boundaries. Working on tomato, Shi et al (2017) found that lateral ablations at the level of organ boundaries are already sufficient to perturb polarity, suggesting some role of these boundaries in organ formation. It is true that we found changes in *pFIL* expression after some of the lateral ablations. However, these changes were always correlated with the comprised outgrowth of leaves. The *FIL* expression domain was reduced in width and even a loss of *pFIL* signals was observed in cases where very few cells were left (Fig.7A-A'). In these cases, we could not unambiguously uncouple growth arrest and the apparent loss of polarity, as both processes occurred simultaneously. When the ablations were slightly further apart, some growth occurred, while in that case *pFIL* also could extend adaxially. This was happening long after growth arrest, however and could be largely indirect. The link between growth and FIL has remained unclear. Eshed et al. (2004) and Goldshmidt et al. (2008) suggest that FIL could be growth promoting, while Refahi et al (2021) did not find a clear correlation between growth rates and *FIL* expression in the flower. Interestingly, ablations of the entire sepal in the flower affected boundary zones outside the domain of *pDRNL* expression, but where the margin promoter *pPRS* was still expressed (Fig. 2B). We have previously shown that margin genes are involved in extending the outgrowing sepal primordium as an important step in maintaining organ flatness (Zhao et al., 2020). We show here that precisely the lateral boundary cells initiate new sepals when the entire organ is ablated. This regeneration process requires PRS, suggesting that under normal conditions the gene maintains the competence of the lateral boundary cells to respecify into a polarized sepal.

In conclusion, we find that in Arabidopsis the local information within and around the primordium is able to withstand major perturbations in local shape and signaling, long before polarity is fully resolved. In this study, we have used three different markers involved in organ initiation and polarity. Extension of this approach to other polarity markers should

provide further insight in how the molecular regulatory network functions and reacts to perturbation.

Materials and methods

Plant material and growth conditions

The mutant (*wox1prs*, (Nakata et al., 2012)) and marker lines (*pFIL: erGFP (Watanabe and Okada, 2003)*, *pDRNL:erGFP* (Cole et al., 2009), *pDRNL:erCERULEAN* (Cole et al., 2013), *pPRS:SV40-3×GFP* (Xu et al., 2015), and *pUBQ10:Lti6b-tdTomato* (Segonzac et al., 2012)) used in this study were described previously. The double or triple fluorescent labeling marker lines were obtained by crossing and subsequently confirmed by antibiotic screening and checking the fluorescence signals. To obtain vegetative shoot apical meristems, plants were grown under short-day conditions on soil (8/16 h light period) for 33-37 days until further dissections. To obtain inflorescence meristems, plants were first cultured in short-day conditions for three weeks and then transferred to long-day conditions (16/8 h light period) for an additional two weeks. Under these conditions, the shoot apical meristems were big enough to facilitate both dissection and laser ablations. Plants grown on soil were cultured with 60% humidity, using light-emitting diodes, 150 $mEm^{-2}s^{-1}$, and at 20–22°C day temperature. For live imaging and long-term culture, the meristems were dissected and cultured *in vitro* on apex culture medium (ACM) (Hamant et al., 2019) supplemented with 200nM N6-Benzyladenine and 0.1% PPM (plant preservative mixture).

Sample preparation

To prepare the vegetative meristems, 33-37-day old rosettes were carefully removed from the soil to preserve the root as much as possible. The rosettes were then washed with water and dried with tissue paper. Whole plants were moved to dissection plates (3% agarose in petri-dish) and immobilized as described by (Shi et al., 2020). To expose the vegetative meristem, the old leaves were cut off as clean as possible using injection needles (0.45mm, BD). The young leaf primordia covering the meristem were dissected away carefully using tweezers under the binocular with big magnification. To prepare inflorescence meristems, the whole shoot apices were inserted in the ACM and dissected with tweezers. After dissection, the inflorescence shoot apices were transferred to a new ACM plate and cultured *in vitro* till further experiments. We usually kept the dissected vegetative and inflorescence meristems recovering around 4 hours prior to imaging and ablations.

Laser ablations

The laser ablation experiments were performed as described in (Zhao et al., 2019), using a Zeiss LSM 700 laser-scanning confocal microscope, equipped with an Andor MicroPoint laser ablation system driven by iQ3 software, which delivered a 6-Hz paused laser at 356 nm. A pre-staining of the meristems with propidium iodide (Sigma, 100 mM) for 5 minutes was carried out to increase the efficiency of laser ablation. To determine the precise site of ablation, we first made an acquisition using Zeiss ZEN software (black edition). We then adjusted the focal plane and chose the circular or freeline tool in iQ3 to draw the trajectory for the ablation according to the position shown in the confocal image. We set the laser power at 8-9 with 5 repetitions for each point on the trajectory in order to make a deep wound. After the ablation, we made another acquisition using the confocal microscope. Under such conditions, our ablations are usually around 2-3 cells deep. In a total of 60 ablations carried out in vegetative meristems, 38 were 2-3 cells deep, 19 3-4 cells deep, and 3 1-2 cells deep.

Live imaging and image processing

For live imaging, the dissected meristems were immersed in distilled water supplemented with 0.1% PPM and examined in a Zeiss LSM 700 laser-scanning confocal microscope equipped with water immersion objectives (W Plan-Apochromat 40x/1.0 differential interference contrast). For three-dimensional image processing, we used the Zeiss ZEN software (black edition) choosing the transparency rendering mode in order to visualize the signals on the meristem/organ primordia surface. Longitudinal optical sections of the stacks were carried out using Fiji freeware.

Acknowledgements

The authors would like to thank Olivier Hamant and Marcus Heisler for kind suggestions on this paper. We would also like to thank Miyuki Nakata and Kiyotaka Okada for providing *pFIL: erGFP* and *wox1 prs* seeds, Wolfgang Werr and John Chandler for providing *pDRNL:erGFP* and *pDRNL:erCERULEAN* seeds, Yuling Jiao and Chuming Liu for providing *pPRS:SV40-3×GFP* seeds. We thank Bihai Shi for instructions on vegetative meristem dissection, Claire Lionnet and PLATIM for supporting the laser ablation experiments. JT and FZ were supported by an ANR-ERA-CAPS grant, Gene2Shape.

Author contributions

F.Z performed the experiments. F.Z. and J.T. conceived the project, analyzed data, and wrote the manuscript.

Conflict of interests

The authors declare no competing interests.

Supporting information

Figures S1-S8.

References

Besnard, F., Refahi, Y., Morin, V., Marteaux, B., Brunoud, G., Chambrier, P., Rozier, F., Mirabet, V., Legrand, J., Lainé, S., et al. (2014). Cytokinin signalling inhibitory fields provide robustness to phyllotaxis. ***Nature*** **505, 417–421.**

Caggiano, M. P., Yu, X., Bhatia, N., Larsson, A., Ram, H., Ohno, C. K., Sappl, P., Meyerowitz, E. M., Jönsson, H. and Heisler, M. G. (2017). Cell type boundaries organize plant development. ***elife*** **6,.**

Chandler, J. W., Cole, M., Flier, A., Grewe, B. and Werr, W. (2007). The AP2 transcription factors DORNROSCHEN and DORNROSCHEN-LIKE redundantly control Arabidopsis embryo patterning via interaction with PHAVOLUTA. ***Development*** **134, 1653–1662.**

Chandler, J. W., Jacobs, B., Cole, M., Comelli, P. and Werr, W. (2011). DORNRÖSCHEN-LIKE expression marks Arabidopsis floral organ founder cells and precedes auxin response maxima. ***Plant Mol. Biol.*** **76, 171–185.**

Cole, M., Chandler, J., Weijers, D., Jacobs, B., Comelli, P. and Werr, W. (2009). DORNROSCHEN is a direct target of the auxin response factor MONOPTEROS in the Arabidopsis embryo. ***Development*** **136, 1643–1651.**

Cole, M., Jacobs, B., Soubigou-Taconnat, L., Balzergue, S., Renou, J. P., Chandler, J. W. and Werr, W. (2013). Live imaging of DORNRÖSCHEN and DORNRÖSCHEN-LIKE promoter activity reveals dynamic changes in cell identity at the microcallus surface of Arabidopsis embryonic suspensions. ***Plant Cell Rep.*** **32, 45–59.**

de Reuille, P. B., Bohn-Courseau, I., Ljung, K., Morin, H., Carraro, N., Godin, C. and Traas, J. (2006). Computer simulations reveal properties of the cell-cell signaling network at the shoot apex in Arabidopsis. ***Proc Natl Acad Sci USA*** **103, 1627–1632.**

Eshed, Y., Izhaki, A., Baum, S. F., Floyd, S. K. and Bowman, J. L. (2004). Asymmetric leaf development and blade expansion in Arabidopsis are mediated by KANADI and YABBY activities. ***Development*** **131, 2997–3006.**

Goldshmidt, A., Alvarez, J. P., Bowman, J. L. and Eshed, Y. (2008). Signals derived from YABBY gene activities in organ primordia regulate growth and partitioning of Arabidopsis shoot apical meristems. ***Plant Cell*** **20, 1217–1230.**

Hamant, O., Das, P. and Burian, A. (2019). Time-Lapse Imaging of Developing Shoot Meristems Using A Confocal Laser Scanning Microscope. ***Methods Mol. Biol.*** **1992, 257–268.**

Heisler, M. G., Ohno, C., Das, P., Sieber, P., Reddy, G. V., Long, J. A. and Meyerowitz, E. M. (2005). Patterns of auxin transport and gene expression during primordium development revealed by live imaging of the Arabidopsis inflorescence meristem. ***Curr. Biol.*** **15, 1899–1911.**

Heisler, M. G., Hamant, O., Krupinski, P., Uyttewaal, M., Ohno, C., Jönsson, H., Traas, J. and Meyerowitz, E. M. (2010). Alignment between PIN1 polarity and microtubule orientation in the shoot apical meristem reveals a tight coupling between morphogenesis and auxin transport. ***PLoS Biol.*** **8, e1000516.**

Hervieux, N., Dumond, M., Sapala, A., Routier-Kierzkowska, A.-L., Kierzkowski, D., Roeder, A. H. K., Smith, R. S., Boudaoud, A. and Hamant, O. (2016). A mechanical feedback restricts sepal growth and shape in ***Arabidopsis*****.** ***Curr. Biol.*** **26, 1019–1028.**

Husbands, A. Y., Chitwood, D. H., Plavskin, Y. and Timmermans, M. C. P. (2009). Signals and prepatterns: new insights into organ polarity in plants. ***Genes Dev.*** **23, 1986–1997.**

Kerstetter, R. A., Bollman, K., Taylor, R. A., Bomblies, K. and Poethig, R. S. (2001). KANADI regulates organ polarity in Arabidopsis. ***Nature*** **411, 706–709.**

Kierzkowski, D., Lenhard, M., Smith, R. and Kuhlemeier, C. (2013). Interaction between meristem tissue layers controls phyllotaxis. ***Dev. Cell*** **26, 616–628.**

Koch, A. J. and Meinhardt, H. (1994). Biological pattern formation: from basic mechanisms to complex structures. ***Rev. Mod. Phys.*** **66, 1481–1507.**

Kuhlemeier, C. and Timmermans, M. C. P. (2016). The Sussex signal: insights into leaf dorsiventrality. *Development* 143, 3230–3237.

McConnell, J. R., Emery, J., Eshed, Y., Bao, N., Bowman, J. and Barton, M. K. (2001). Role of PHABULOSA and PHAVOLUTA in determining radial patterning in shoots. *Nature* 411, 709–713.

Nakata, M., Matsumoto, N., Tsugeki, R., Rikirsch, E., Laux, T. and Okada, K. (2012). Roles of the middle domain-specific WUSCHEL-RELATED HOMEOBOX genes in early development of leaves in Arabidopsis. *Plant Cell* 24, 519–535.

Qi, J., Wang, Y., Yu, T., Cunha, A., Wu, B., Vernoux, T., Meyerowitz, E. and Jiao, Y. (2014). Auxin depletion from leaf primordia contributes to organ patterning. *Proc Natl Acad Sci USA* 111, 18769–18774.

Refahi, Y., Zardilis, A., Michelin, G., Wightman, R., Leggio, B., Legrand, J., Faure, E., Vachez, L., Armezzani, A., Risson, A.-E., et al. (2021). A multiscale analysis of early flower development in Arabidopsis provides an integrated view of molecular regulation and growth control. *Dev. Cell* 56, 540-556.e8.

Reinhardt, D., Pesce, E.-R., Stieger, P., Mandel, T., Baltensperger, K., Bennett, M., Traas, J., Friml, J. and Kuhlemeier, C. (2003). Regulation of phyllotaxis by polar auxin transport. *Nature* 426, 255–260.

Reinhardt, D., Frenz, M., Mandel, T. and Kuhlemeier, C. (2005). Microsurgical and laser ablation analysis of leaf positioning and dorsoventral patterning in tomato. *Development* 132, 15–26.

Sawa, S., Watanabe, K., Goto, K., Liu, Y. G., Shibata, D., Kanaya, E., Morita, E. H. and Okada, K. (1999). FILAMENTOUS FLOWER, a meristem and organ identity gene of Arabidopsis, encodes a protein with a zinc finger and HMG-related domains. *Genes Dev.* 13, 1079–1088.

Scanlon, M. J., Schneeberger, R. G. and Freeling, M. (1996). The maize mutant *narrow sheath* fails to establish leaf margin identity in a meristematic domain. *Development* 122, 1683–1691.

Segonzac, C., Nimchuk, Z. L., Beck, M., Tarr, P. T., Robatzek, S., Meyerowitz, E. M. and Zipfel, C. (2012). The shoot apical meristem regulatory peptide CLV3 does not activate innate immunity. *Plant Cell* 24, 3186–3192.

Shi, J., Dong, J., Xue, J., Wang, H., Yang, Z., Jiao, Y., Xu, L. and Huang, H. (2017). Model for the role of auxin polar transport in patterning of the leaf adaxial-abaxial axis. *Plant J.* 92, 469–480.

Shi, B., Wang, H. and Jiao, Y. (2020). Live imaging of arabidopsis axillary meristems. *Methods Mol. Biol.* 2094, 59–65.

Siegfried, K. R., Eshed, Y., Baum, S. F., Otsuga, D., Drews, G. N. and Bowman, J. L. (1999). Members of the YABBY gene family specify abaxial cell fate in Arabidopsis. *Development* 126, 4117–4128.

Snow, R. and Snow, M. (1954a). Experiments on the cause of dorsiventrality in leaves. *Nature* 173, 644–644.

Snow, R. and Snow, M. (1954b). Experiments on the cause of dorsiventrality in leaves. *Nature* 174, 352–353.

Sussex, I. M. (1951). Experiments on the cause of dorsiventrality in leaves. *Nature* 167, 651–652.

Tameshige, T., Fujita, H., Watanabe, K., Toyokura, K., Kondo, M., Tatematsu, K., Matsumoto, N., Tsugeki, R., Kawaguchi, M., Nishimura, M., et al. (2013). Pattern dynamics in adaxial-abaxial specific gene expression are modulated by a plastid retrograde signal during Arabidopsis thaliana leaf development. *PLoS Genet.* 9, e1003655.

Watanabe, K. and Okada, K. (2003). Two discrete cis elements control the Abaxial side-specific expression of the FILAMENTOUS FLOWER gene in Arabidopsis. *Plant Cell* 15, 2592–2602.

Xu, T.-T., Ren, S.-C., Song, X.-F. and Liu, C.-M. (2015). CLE19 expressed in the embryo regulates both cotyledon establishment and endosperm development in Arabidopsis. *J. Exp. Bot.* 66, 5217–5227.

Yamaguchi, T., Nukazuka, A. and Tsukaya, H. (2012). Leaf adaxial-abaxial polarity specification and lamina outgrowth: evolution and development. *Plant Cell Physiol.* 53, 1180–1194.

Zhang, C., Wang, J., Wenkel, S., Chandler, J. W., Werr, W. and Jiao, Y. (2018). Spatiotemporal control of axillary meristem formation by interacting transcriptional regulators. *Development* 145,.

Zhao, F., Chen, W., Sechet, J., Martin, M., Bovio, S., Lionnet, C., Long, Y., Battu, V., Mouille, G., Monéger, F., et al. (2019). Xyloglucans and microtubules

synergistically maintain meristem geometry and phyllotaxis. *Plant Physiol.* 181, 1191–1206.

Zhao, F., Du, F., Oliveri, H., Zhou, L., Ali, O., Chen, W., Feng, S., Wang, Q., Lü, S., Long, M., et al. (2020). Microtubule-Mediated Wall Anisotropy Contributes to Leaf Blade Flattening. *Curr. Biol.* 30, 3972-3985.e6.

Zhu, M., Chen, W., Mirabet, V., Hong, L., Bovio, S., Strauss, S., Schwarz, E. M., Tsugawa, S., Wang, Z., Smith, R. S., et al. (2020). Robust organ size requires robust timing of initiation orchestrated by focused auxin and cytokinin signalling. *Nat. Plants* 6, 686–698.

Figures

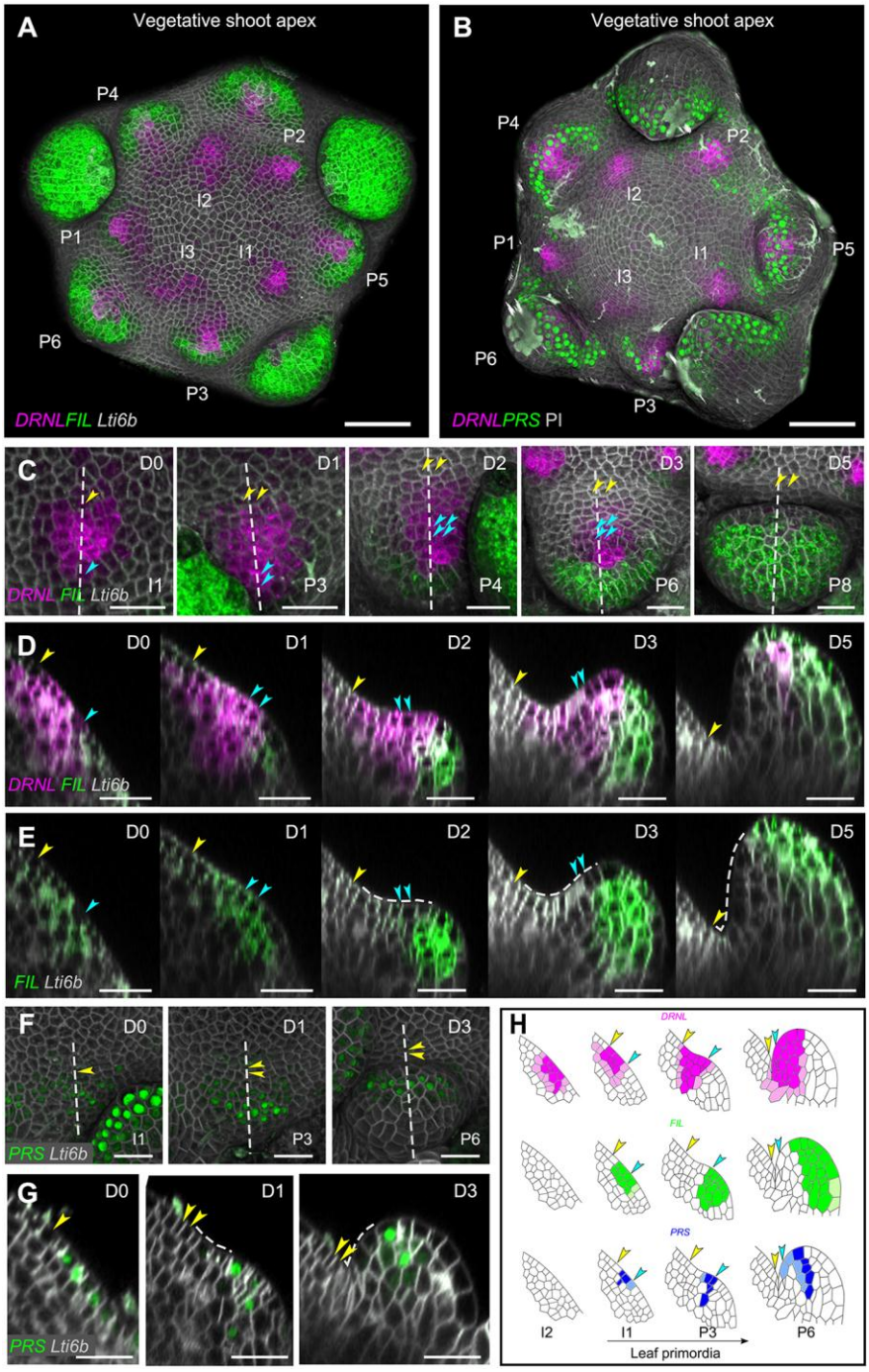

Figure 1. Dynamic gene expression pattern in vegetative shoot apices.

(A-B) Top view of 3D reconstruction of vegetative shoot apices co-expressing *pDRNL:erCERULEAN/ pFIL:erGFP/ pUBQ10:TdTomato-Lti6b* (A) *and pDRNL:erCERULEAN/ pPRS:SV40-3×GFP* (B). The stages of leaf primordia are marked according to the phyllotactic patterning (from I_3 to P_6). The dissected old primordia were trimmed off from the projections for clarity. **(C-E)** Kinetics of *pDRNL* and *pFIL* expression in leaf primordia. The growth of an I_1 initium was followed for five days (Day 0 (D0) to Day 5 (D5)). (C) Top view of 3D reconstructions. The approximate stages of leaf primordium are shown on the right bottom (I_1 to P_8) according to Fig.S1. (D-E) Longitudinal sections of (C) represented with different fluorescent channels. The sections were along the dashed lines as indicated in (C). Arrowheads mark the same cell and its descendants. Note that *pFIL* expression overlaps with *pDRNL* at the beginning, and gradually shifts towards the abaxial side of leaf primordium. By contrast, *pDRNL* is sustained in the adaxial side of leaf primordium. In P_8, *pDRNL* signal is only concentrated at the tip of leaf primordia. The dashed lines shown in (E) indicate the enlargement of the adaxial domain. **(F-G)** Kinetics of *pPRS* expression in leaf primordia followed for 3 days. (F) Top views of 3D reconstructed images. The approximate primordium stages are indicated (I_1 to P_6) according to Fig.S1. (G) Longitudinal sections along the dashed lines in (F). Yellow arrowheads mark the same cell and its descendants. The adaxial domain is indicated by dashed lines. **(H)** Schematic representation of dynamic gene expression patterns in longitudinal sections of leaf primordia at different stages. Arrowheads indicate the cell lineages. Scale bars: 20µm. See also Figure S1 and S2.

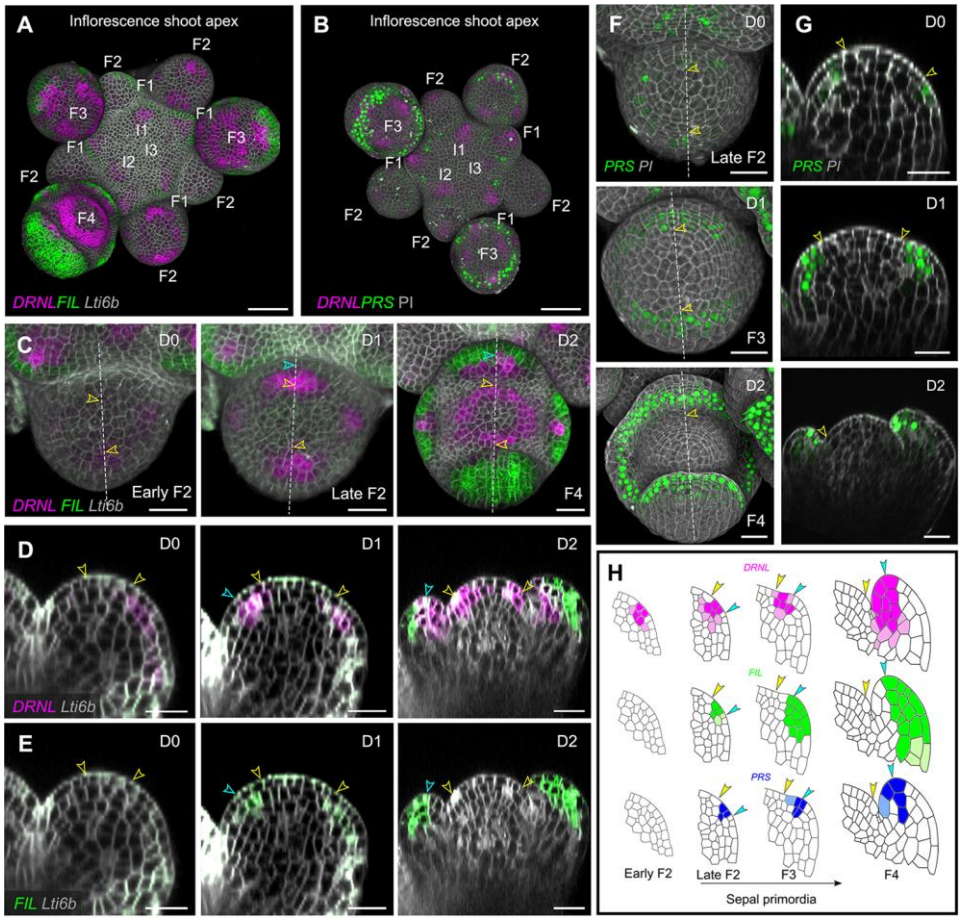

Figure 2. Dynamic gene expression pattern in inflorescence shoot apices.

(A-B) Top view of the 3D reconstruction of inflorescence shoot apices expressing *pDRNL:erCERULEAN/pFIL:erGFP/pUBQ10:TdTomato-Lti6b* (A) and

pDRNL:erCERULEAN/ pPRS:SV40-3×GFP (B). The successive initia are marked from I_3 to I_1, the floral buds at stage 1, 2, 3 and 4 are marked as F1, 2, 3 and 4. **(C-E)** Kinetics of *pDRNL* and *pFIL* expression in a floral bud (at early stage 2) followed for two days, developing from stage 2 to stage 4. (C) Top view of 3D reconstruction images. (D-E) Longitudinal sections along the dashed line in (C) showing different fluorescent signals. Arrowheads mark the limits of a group of cells and its descendants. Note that *pFIL* is activated after *pDRNL*. The initial *pFIL* expression overlaps with *pDRNL*, and gradually locates at the abaxial side of the sepal primordium. On the contrary, *pDRNL* signals remain on the adaxial side. (**F-G**) Kinetics of *pPRS* expression in stage 2 floral bud followed for 2 days. (F) Top views of 3D reconstructions. (G) Longitudinal sections along the dashed line shown in (F). Arrowheads mark the cell and its descendant. **(H)** Schematic representation of dynamic gene expression patterns in sepal primordia from stage 2 to stage 4, Arrowheads indicate the cell lineages. Scale bars: 20μm. See also Figure S3.

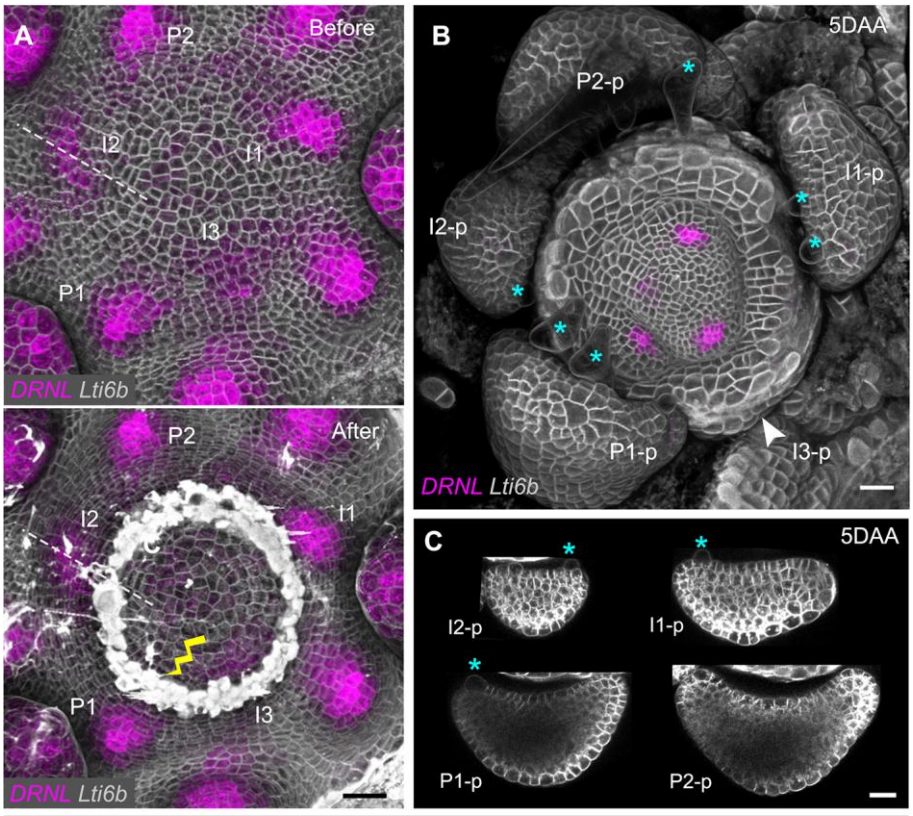

E

Longitudinal view	Positions	Phenotypes (n)	
		flat	radial
VM; DRNL; Ablations	I_1	10	0
	I_2	8	0
	I_3	4	0

Longitudinal view	Positions	Phenotypes (n)	
		flat	radial
VM; DRNL; Ablations	P_1	12	0
	P_2	10	0

Figure 3. Circular ablation next to initia or primordia in vegetative meristems do not perturb polarity.

(A) Top view of 3D reconstruction of vegetative shoot apex expressing *pDRNL:erCERULEAN* and *pUBQ10:TdTomato-Lti6b* before (upper panel) and after (lower panel) laser ablation. The age of leaf primordia is indicated as I_3-P_2. The wound caused by ablation is indicated by the yellow lightning sign. **(B)** Top view of the vegetative meristem at five days after ablation (5DAA). The growth of leaf primordia shown in (A) was followed and marked as I_3-p to P_2-p referring to the original I_3 to P_2-positions. Note that a distal part of

I_3 was ablated after which only limited outgrowth in the form of a ring formed (indicated by white arrowhead) and *pDRNL* activity was lost. **(C)** Cross-sections of I_2-p to P_2-p in (B), showing the flattening of these leaves. The adaxial cell fate is characterized by the formation of trichomes, indicated by blue stars in (B) and (C). **(D)** Growth dynamics of the I_2 initium during 3 days after ablations, represented by longitudinal sections along the dashed lines shown in (A and B). The wound is marked with the yellow lightning sign and arrowheads. Note that the circular ablation did not change the expression pattern of *pDRNL*. (**E**) Summary of the wounding position and corresponding phenotypes after circular ablations next to individual initia/primordia in vegetative meristems (VM) after 5DAA. Scale bars: 20µm. See also Figure S4 and S5.

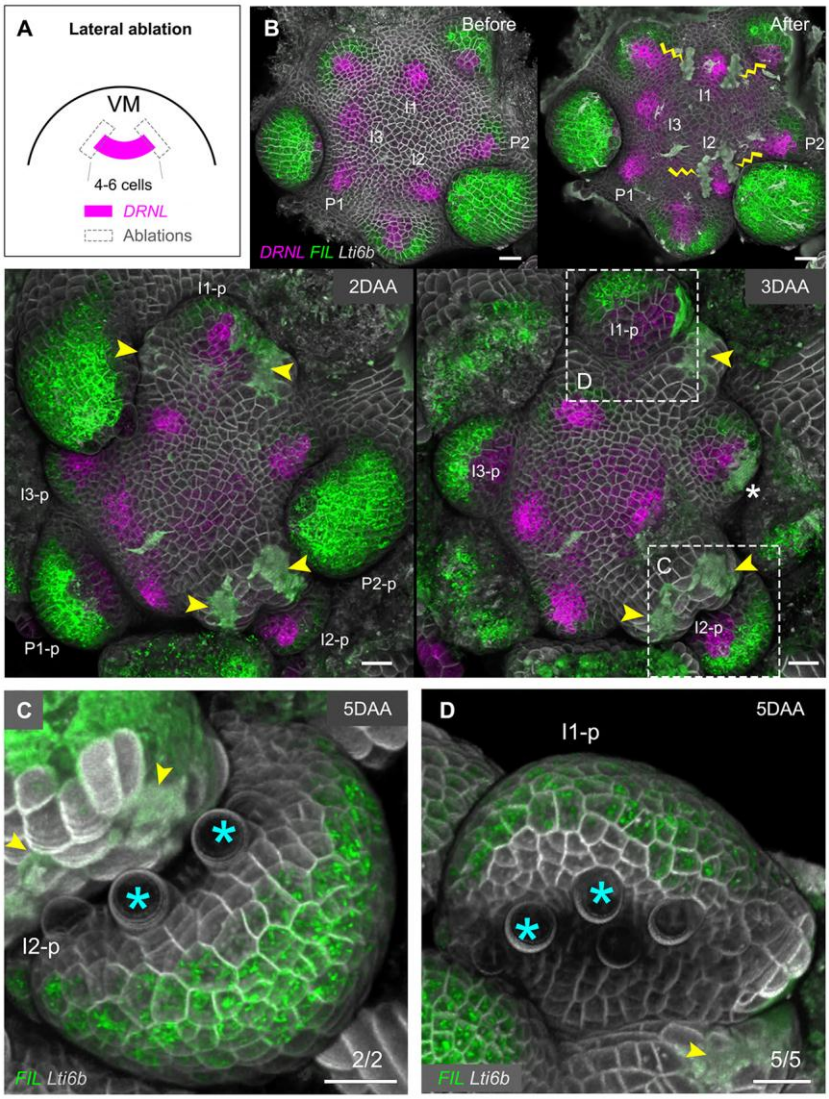

Figure 4. Lateral ablation in vegetative meristems next to or marginally touching the initia and primordia do not perturb polarity

(A) Schematic representation of the lateral ablations in vegetative meristem (VM). **(B)** Overview of representative vegetative meristem before and after laser ablation. The growth of the meristem was followed for 5 days. The wounds are marked by yellow lightning signs and arrowheads. The initial stages of leaf primordia just before or after ablation are indicated by I_3 to P_2, their respective later stages as I_3-p to P_2-p as in Fig. 3. The wound marked by a white star on 3DAA was caused by dissecting away P_2-p at 2DAA. **(C-D)** Detailed shapes of I_2-p and I_1-p (dashed frames in B) at 5DAA. The trichomes initiated from the adaxial leaf surface are marked with blue stars. Scale bars: 20µm.

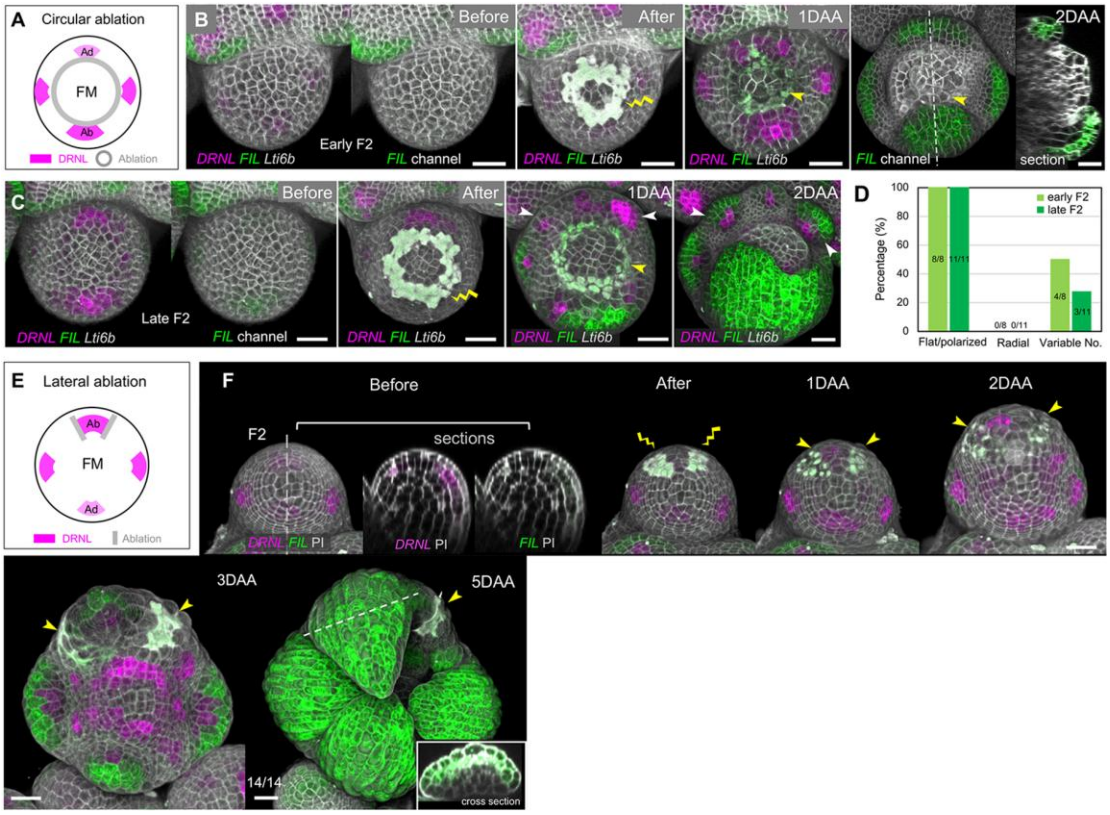

Figure 5. Ablations in floral meristems.

(A) Schematic representation of the circular ablation strategy in floral meristem (FM). The outer (Abaxial) and inner (Adaxial) sepal initia are marked as Ab and Ad respectively. **(B)** A representative example of circular ablation in early stage 2 floral bud (Early F2). The growth of the floral bud was followed for 2 days. Note that *pFIL* was not activated yet before the ablation. The wounds are marked by the yellow lightning sign and arrowheads. **(C)** A representative example of circular ablation in late stage 2 floral bud (Late F2), when the *pFIL* starts to be activated. White arrowheads indicate the ectopically initiated sepal primordia. Note that in all cases shown in (B and C), circular ablation did not affect the sepal polarity. **(D)** Quantitative summary of (B-C) on sepal shape/polarity formation. **(E)** Schematic representation of the lateral ablation strategy in floral meristem. The outer (Ab) sepal primordia in stage 2 floral buds were confined by two lateral incisions. **(F)** A representative example of lateral ablations in a stage 2 floral bud. Note that at this stage, the *pFIL* activity was barely visible before the ablation. The wounds are marked by yellow lightning signs and arrowheads. After the ablations, the growth was followed for 5 days and polarity was not compromised in 14/14 primordia. Scale bars: 20µm.

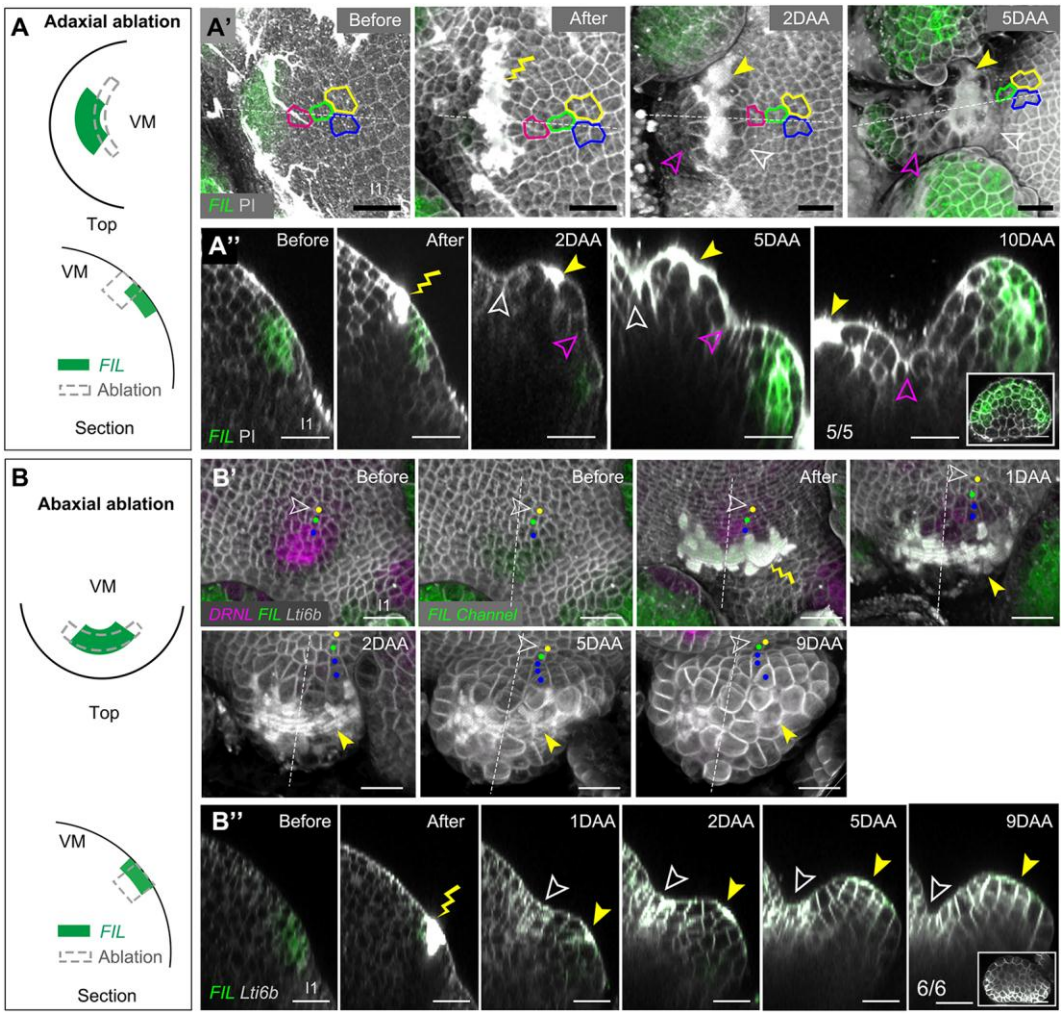

Figure 6. Ablations parallel to meristem circumference, within leaf initia/primordia

(A-A'') Ablations of the adaxial part of the *pFIL* expression domain before *pFIL* polarizes. (A) Schematic representation of the wounding position from a top (upper panels) and longitudinal section view (lower panels). (A') Top view of a vegetative meristem showing an example of I_1 leaf initium before and up to 5 days after ablation. The precise wounding sites are marked with yellow lightning signs or arrowheads. Cell lineages are marked with different colors. (A'') Longitudinal sections of the same primordium along the dashed lines in (A'). At 2DAA *pFIL* activity is substantially reduced. The initial organ boundary starts to fold (open arrowhead), while a bulge starts to grow out, and an additional boundary is defined (magenta arrowhead). After ten days a polarized leaf with abaxial *pFIL* labeling is formed. Cross section of the leaf in insert. The same results were obtained from 5 different I_1 or P_1. **(B-B'')** Ablations including most of the abaxial *pFIL/pDRNL* expression domain. (B) Schematic representation of the wounding position from a top (upper panels) and longitudinal section (lower panels). (B') Outgrowth after ablation at I_1 position. A small outgrowth is formed after

9 days. The color dots show cell lineage (B'') Longitudinal sections along the dashed lines in the same sample showing that *pFIL* activity is lost in the outgrowth. The inset shows the transverse sections of the outgrowth at 9DAA. The wounding sites are marked with the yellow lightning sign or yellow arrowheads. White hollow arrowheads indicate organ boundary. The Same results were obtained from 6 I_1 or P_1. Scale bars: 20μm.

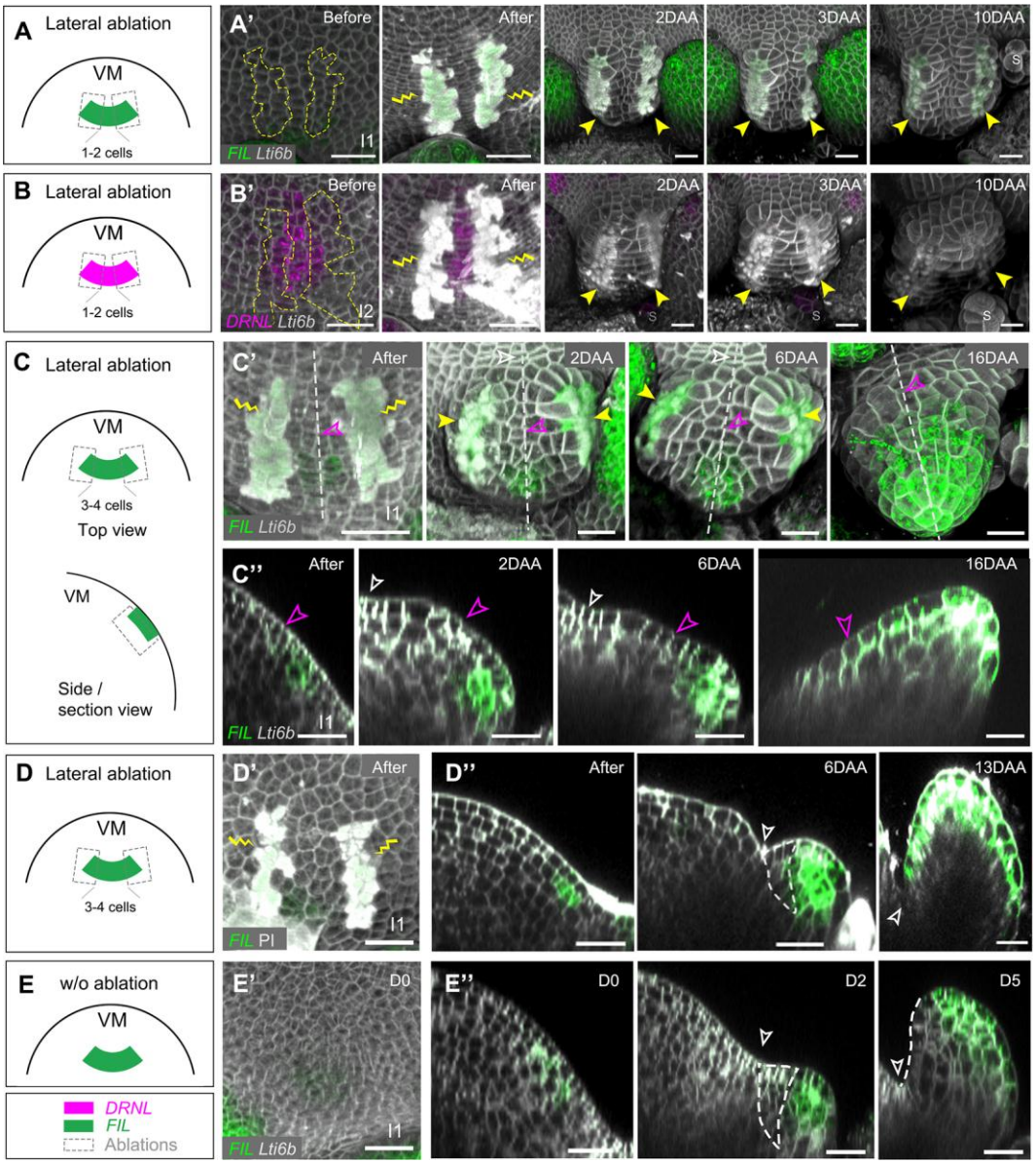

Figure 7. lateral ablations within leaf initia.

(A-B') Lateral ablations leaving a row of 1~2 initium cells intact lead to the inhibition of leaf outgrowth in I_1(A-A') and I_2 (B-B') and loss of *pFIL* and *pDRNL* expession. (A and B) Schematic representation showing the positions of the ablations. (A' and B') Top views of representative ablations. The same results were obtained from 2 I_1 and 2 I_2 leaf initia. The wounds are marked by yellow lightning signs and arrowheads. The contours of the corresponding ablation zones are indicated in the left panel (before ablation) of (A') and (B'). "S" in the right panels indicates the newly initiated stipules. **(C-C'')** A representative example of lateral ablation (of 3-4 cells apart) at I_1 showing reduced growth from 0-16 DAA. (C) Schematic representation showing the wounding positions. (C') Top view (C'') Longitudinal sections along the dashed lines shown in (C') Hollow magenta arrowheads mark

the same cell wall over time. Polarity is not perturbed up to 6DAA, but then leads to the formation of a small abaxialized structure after 16 days with *pFIL* activity extending adaxially beyond the magenta mark. Yellow lightning signs mark the wounding sites. **(D-D'')** Another example of a lateral ablation (of 3-4 cells apart) at I_1. (D) Schematic showing the wounding position. (D') Top view. (D'') Longitudinal sections showing leaf growth for 13 days. Yellow lightning signs: wounding sites. Hollow white arrowheads: organ boundaries. White dashed lines indicate the adaxial domains. **(E-E'')** The development of a control leaf without wounding. (E) The schematic of the leaf initial in the intact meristem. (E') Top view of a typical I_1 leaf initium. (E'') Longitudinal sections showing the leaf growth for 5 days. White dashed lines indicate the adaxial domains. Scale bars: 20μm. See also Figure S7.

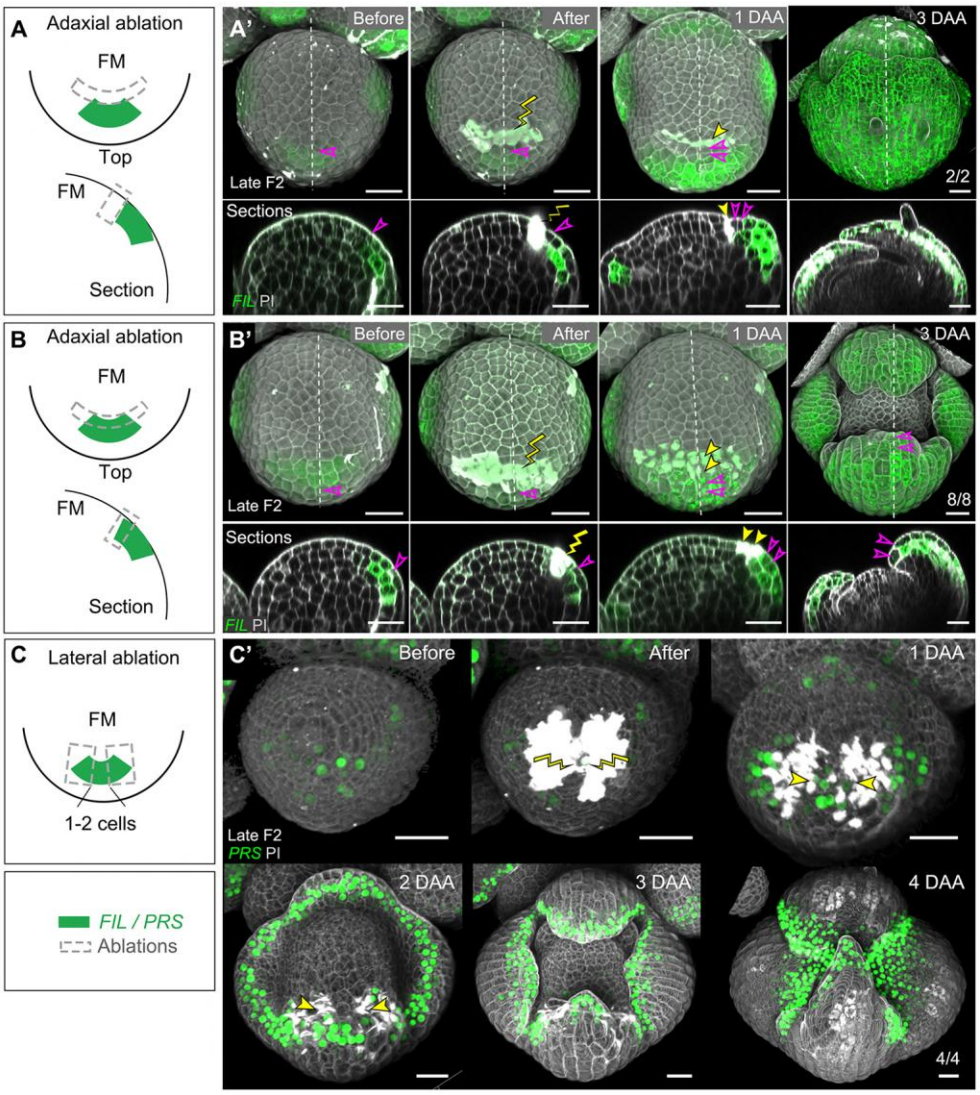

Figure 8. Ablations parallel to the meristem circumference, within sepal initia.

(A and A') Ablation next to the *pFIL* domain. (A) shows the schematic representation, (A') a typical example showing normal sepal development. Upper panels top views, lower panels longitudinal sections along dotted lines. **(B and B')** Ablation eliminating the adaxial part of the *pFIL* labelled domain. (B) shows the schematic representation, (B') a typical example showing normal sepal development. Upper panels top views, lower panels longitudinal sections along dotted lines. **(C-C')** Lateral ablation in stage 2 floral bud expressing the *pPRS:SV40-3×GFP* marker. (C) Schematic representation showing the wounding position. Growth was followed for 4 days and a flat sepal was formed. Note that only a single cell was left in between the wounds. The wounds are indicated by yellow lightning signs and arrowheads. Magenta arrowheads mark the cell next to the wound and its descendants. Scale bars: 20µm.

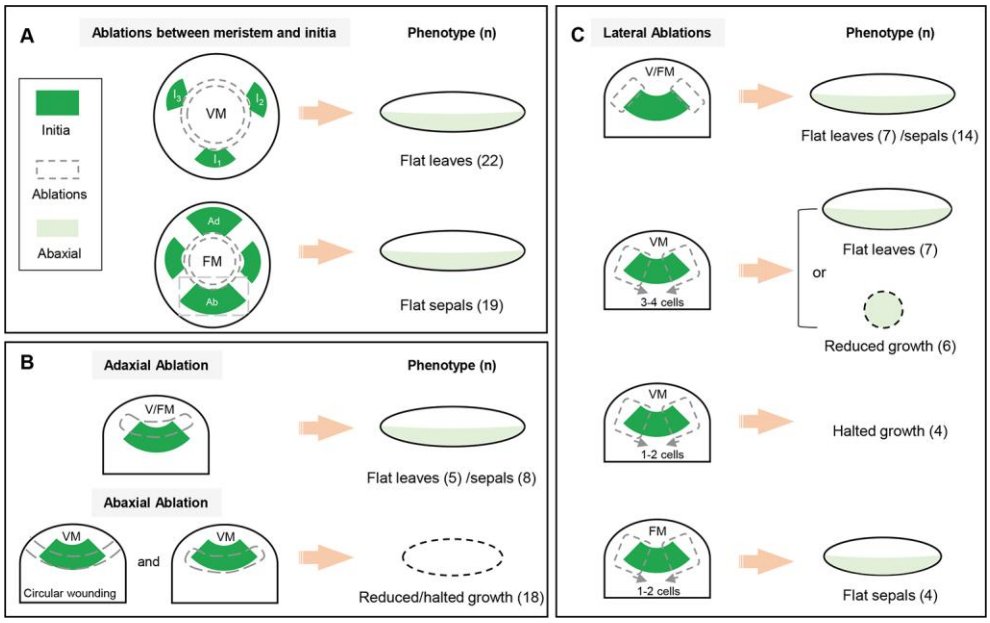

Figure 9. Schematic representations of laser ablations.

(**A**) A number of circular ablations did not, or just touched marginally of the leaf initia (at VM) and sepals (at FM). These systematically developed into flat shapes with normal polarity. (**B**) The killing of adaxial parts of young initia does not perturb organ polarity in VM and FM (upper panel). The wounds in the abaxial part of young initia cause reduced or halted organ growth in VM (lower panel). (**C**) Lateral ablations which leave a large area of initia/primordia intact do not perturb organ flatness and polarity in VM and FM (upper panel). When the wounds are kept 3-4 cells apart in the leaf initia, the leaves will become flat or show a dramatically reduced final size which can be abaxialized after longer periods. The leaf initia will stop growing when the wounds are only 1-2 cells apart in the VM (middle panels). However, even if only 1-2 sepal initia cells are left after wounding, flat sepals are still able to grow out (lower panel).

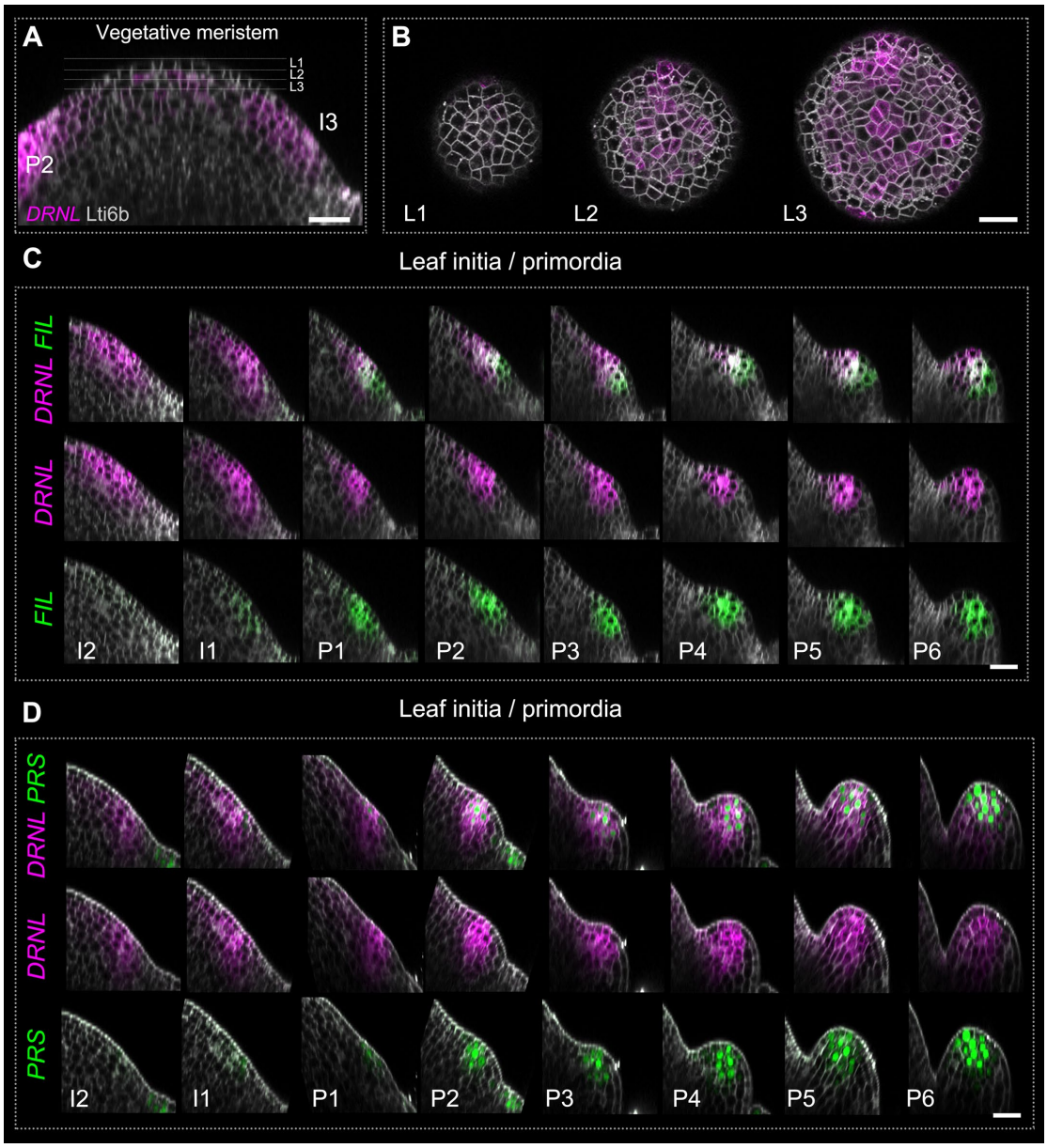

Figure S1. Gene expression pattern in leaf initia/primordia. Related to Figure 1.

(**A**) *pDRNL* activity in the longitudinal section of vegetative meristem.

(**B**) The top view of the *pDRNL* signals at different cell layers from the meristem dome, showing very patchy expression of *DRNL* in L2 and L3 layers. The cross-sections were along the cell planes indicated in (A).

(**C**) Longitudinal sections of leaf initia/primordia from I_2 to P_6. This developmental

series is taken from the same meristem at the same time point. *pDRNL* is initially activated in a large area at the flank of the meristem, then is restricted to the adaxial and middle domain of the leaf primordia from P_1 onwards until P_6. On the contrary, *pFIL* expression initially mostly overlaps with *pDRNL* and then gradually shifts abaxially from P_1 onwards. At P_6, *pFIL* signals are located at the abaxial and middle domains. (**D**) Longitudinal sections of leaf initia/primordia from I_2 to P_6 showing the colocalization of *pDRNL* and *pPRS*. *pPRS* is initially activated within the *pDRNL* domain at I_1. Later on, *pPRS* signals shift from the adaxial to the middle domain (from P_1 to P_4) and remain restricted to the ad-abaxial boundary. Scale bars: 20µm.

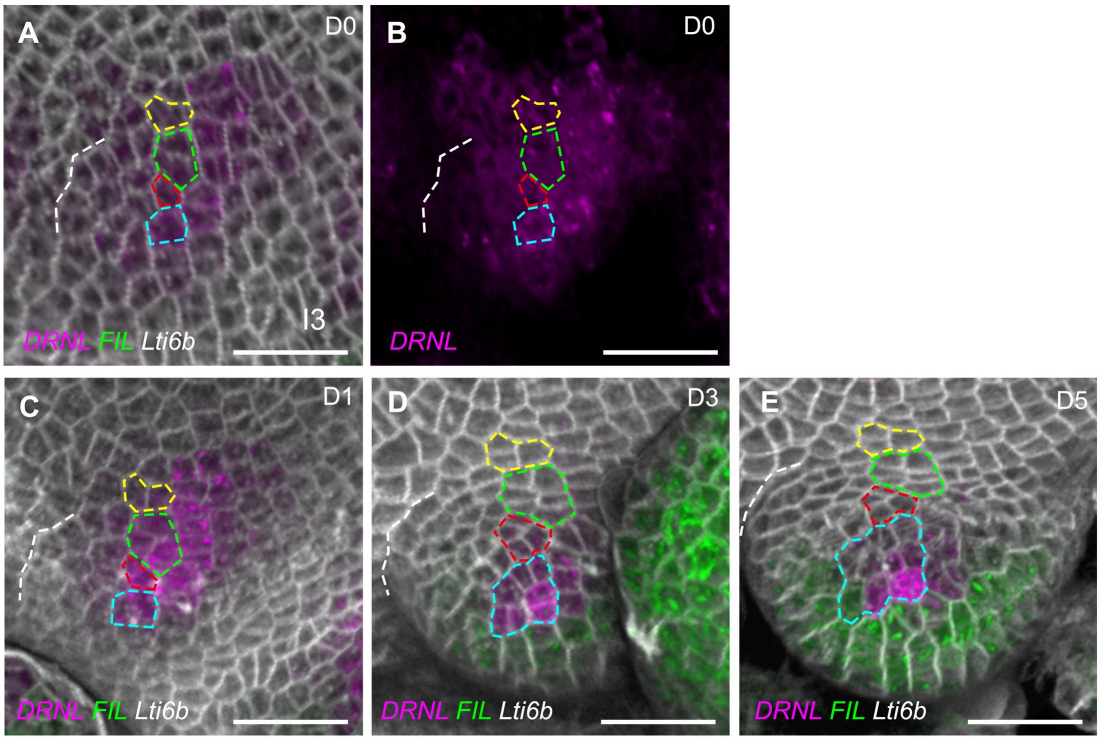

Figure S2. Detailed cell lineage tracking at I_3 position in vegetative meristem. Related to Figure 1.

(**A**) Top view of 3D reconstruction of I_3 leaf initium expressing *pDRNL*, *pFIL* and membrane markers.

(**B**) *DRNL* channel of image in (A).

(**C-E**) The growth of the I_3 initium tracked for five days. Sister cells are surrounded by colored dotted lines. The dashed white line represents the lateral boundary of the leaf initium/primordium. Scale bars: 20μm.

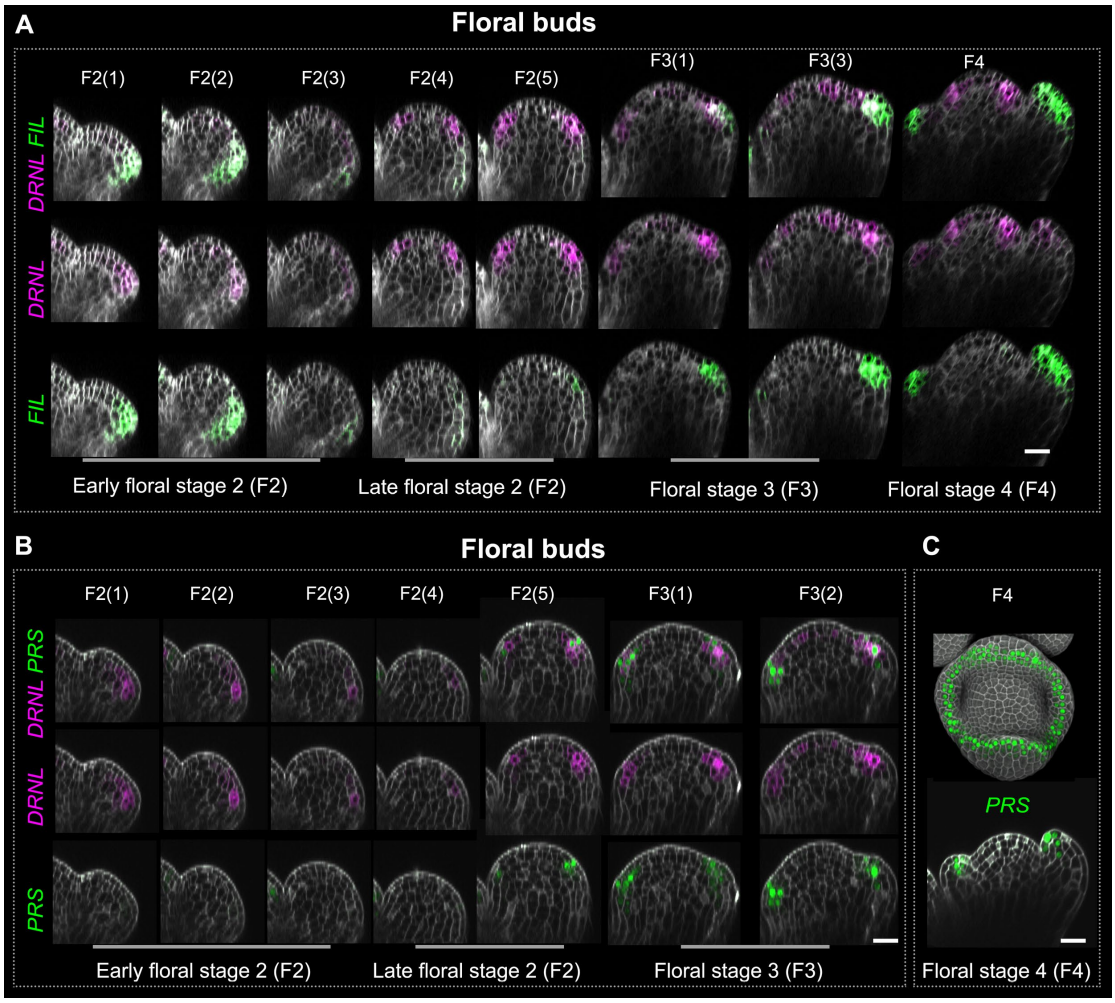

Figure S3. Gene expression pattern in floral buds. Related to Figure 2.

(**A**) Longitudinal sections of floral buds from stage 2 to stage 4 with detailed subdivisions (e.g. F2(1), F2(2) etc.). Developmental series taken from the same inflorescence. During early stage 2, the *pDRNL* and *pFIL* activation domains are largely overlapping in the cryptic bract. *pDRNL* and *pFIL* are gradually repressed in the cryptic bract, to be fully switched off at the beginning of late stage 2. At the same time, *pDRNL* is activated in sepal initia. As in the leaf, *pDRNL* signals are gradually restricted to the adaxial domain during floral stage 3, and to the sepal tip at floral stage 4. *pFIL* activity initially mostly overlaps with the *pDRNL* domain and then becomes more abaxial at floral stage 3 During floral stage 3, *pFIL* expression gradually shifts abaxially, and becomes located at the abaxial and middle domains at floral stage 4.

(**B**) Longitudinal sections of floral buds from stage 2 to stage 3. Note that there is no detectable *pPRS* signal in the cryptic bract during early stage 2. *pPRS* is activated during

late floral stage 2 in the future sepal, then becomes gradually restricted to the adaxial domains during floral stage 3.

(**C**) *pPRS* signals in stage 4 floral bud in 3D (upper panel) and section (lower panel). The *pPRS* signal finally shifts to the middle domain of the sepal at floral stage 4 (lower panel). Note that *pPRS* is also active in lateral sepal boundaries. Scale bars: 20μm.

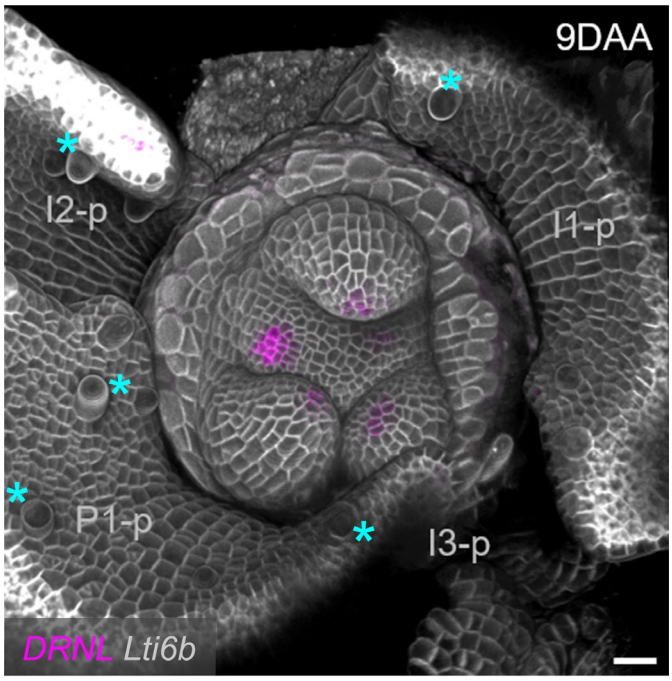

Figure S4. Architecture of vegetative meristem and leaf development at nine days after circular ablations. Related to Figure 3.

Top view of the vegetative meristem shown in Fig. 3 at nine days after ablation (9DAA). The ablation has caused a ring-like outgrowth. Note that leaves next to the ablation at the I_1 to P_1 positions (I_1-p to P_1-p) developed a clear polarity with trichomes (blue stars) on the adaxial side and have grown substantially (compare with Fig. 3B). New primordia (expressing *pDRNL:erCERULEAN)* are forming inside the healed wound. There was no leaf formed at I_3 position (I_3-p). Scale bar: 20µm.

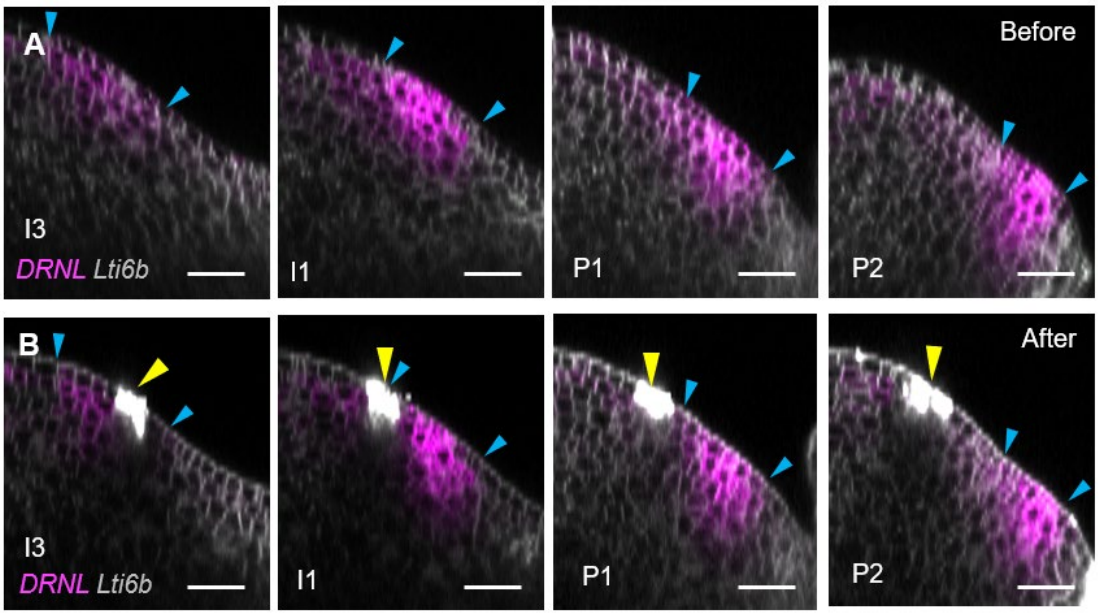

Figure S5. Wounding positions after circular ablations in the vegetative meristem shown in Figure 3.

(**A-B**) Longitudinal sections at different positions in the meristem (shown in Figure 3A) before (A) and after ablation (B). The wounds are indicated by yellow arrowheads. The expression domains of *pDRNL* are indicated by blue arrowheads. Scale bars: 20µm.

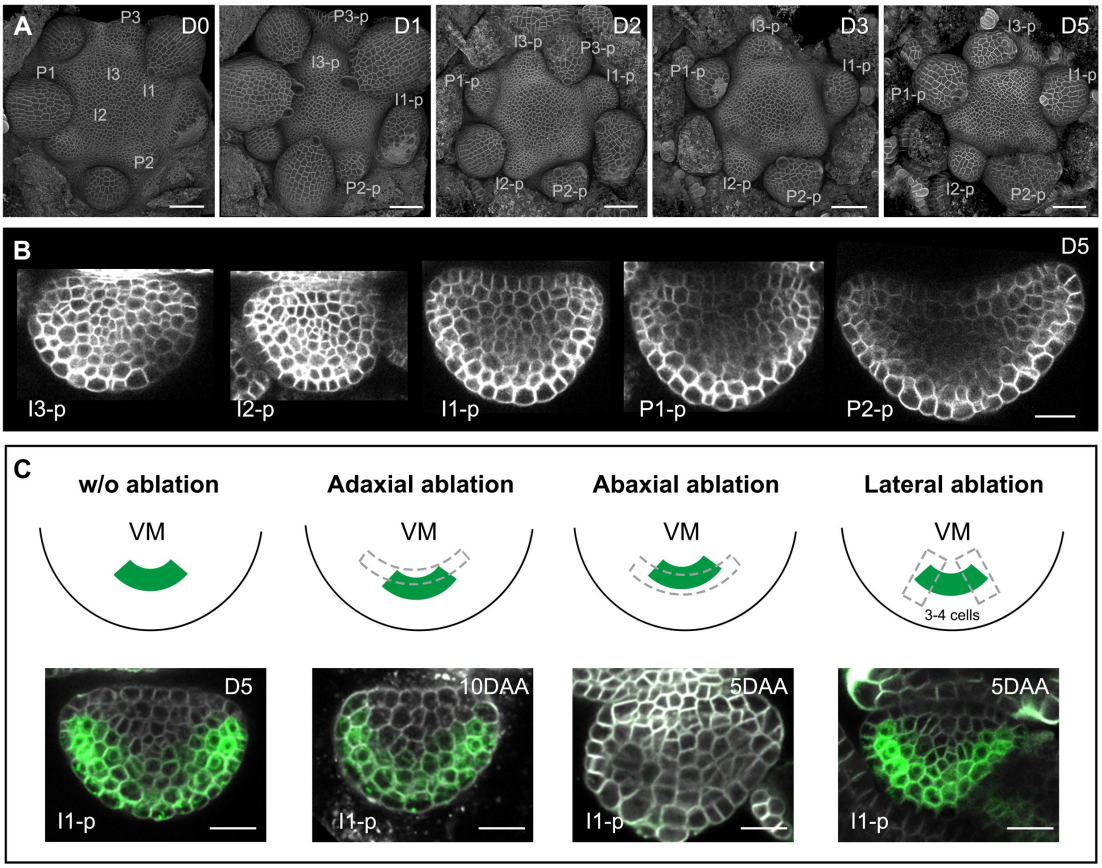

Figure S6. Leaf shape and polarity in intact and wounded vegetative meristems.

(**A**) A representative intact vegetative meristem cultured *in vitro* for 5 days.

(**B**) Cross-sections of leaf primordia at different positions on day 5.

(**C**) leaf polarity in control and after different types of ablations. The abaxial identity is marked by *pFIL* signals (green). Scale bars: 50μm in (A); 20μm in (B and C).

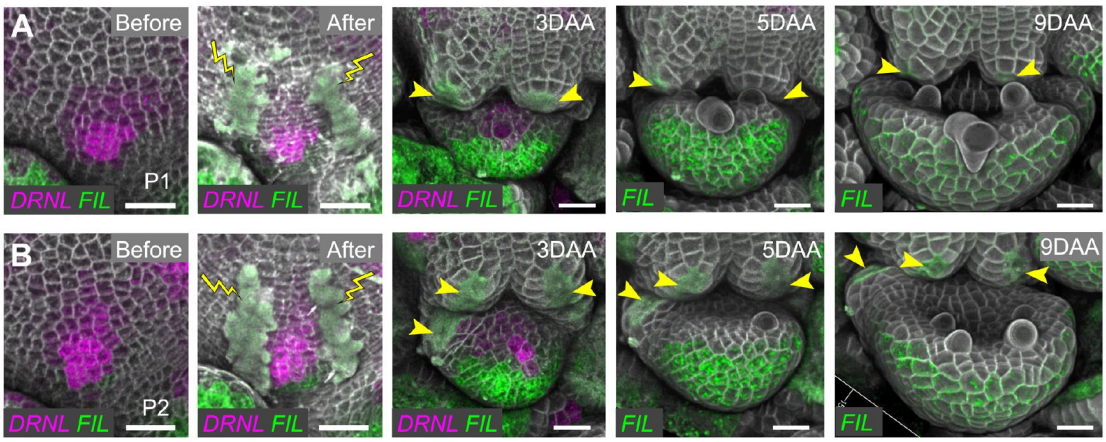

Figure S7. Lateral ablations at P1 and P2. Related to Figure 4.

(A-B) Representative lateral ablations at P1 (A) and P2 (B), 4-5 cells wide. The wounds are marked by yellow lightning signs and arrowheads. After the ablations, the growth was followed for 9 days Scale bars: 20µm.

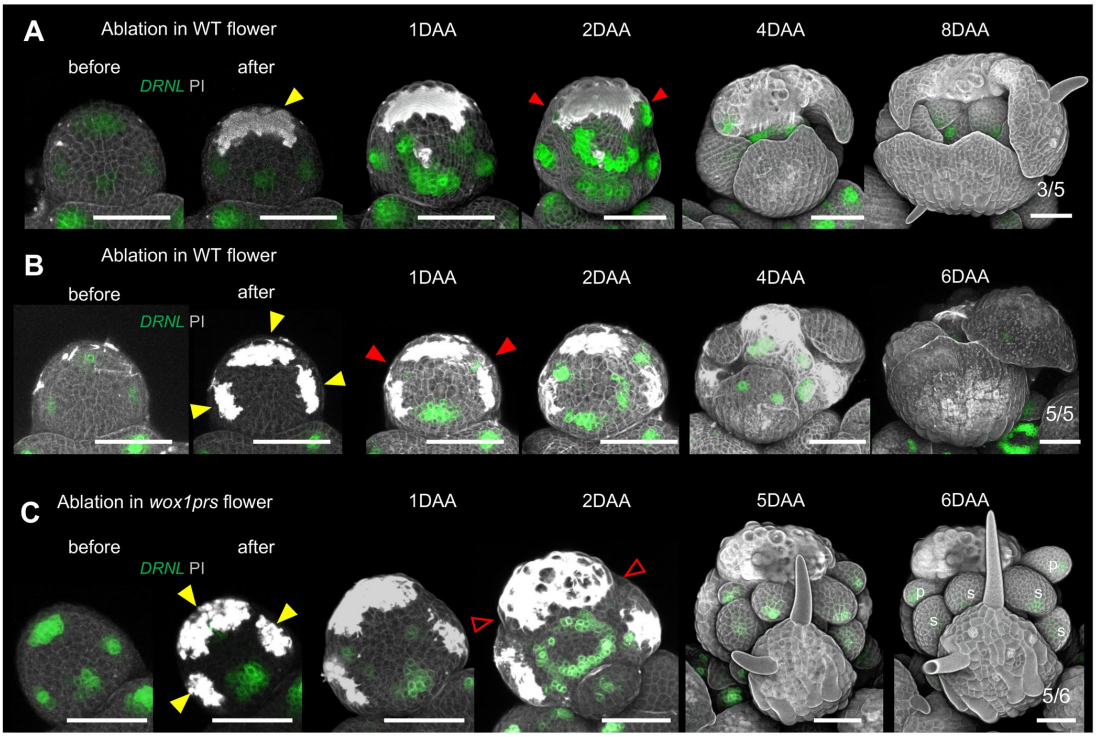

Figure S8. Regeneration of sepal primordia requires *WOX1/PRS* activity.

(**A**) When founder cells (indicated by *pDRNL:erGFP*) of the outer sepal were killed, new founder cells were regenerated from two lateral boundaries of the eliminated primordia (red arrowheads). (**B**) The elimination of founder cells of the outer and two lateral sepals in wild type flowers. The regeneration occurs de novo at lateral boundaries (red arrowheads) indicating that regeneration is not induced by the signal from neighboring sepal primordia. The same results were obtained from 5 different floral buds.

(**C**) The elimination of founder cells of the outer and two lateral sepals in a *wox1 prs* flower. There is no regeneration of new sepal primordia at lateral boundaries (hollow red arrowheads). p, petal; s, stamen. The same results were obtained from 5 meristems. The wounds are marked by yellow arrowheads in (A-C). Scale bars: 50μm.